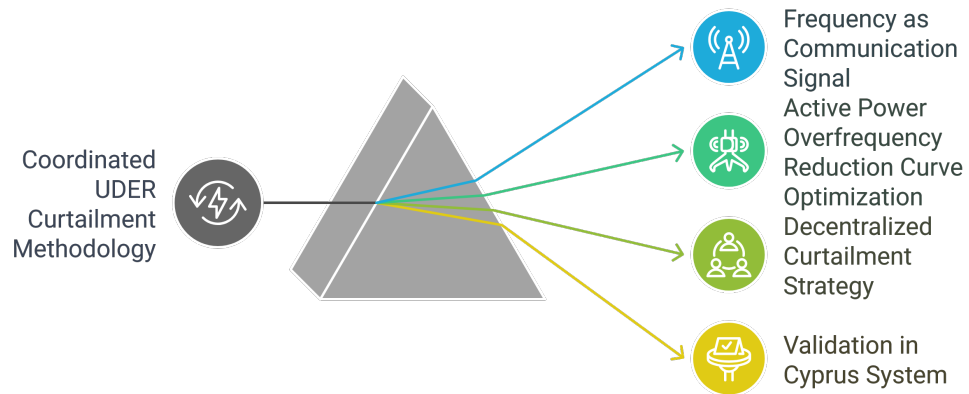


# Graphical Abstract

## Coordinated Curtailment of Uncontrollable Distributed Energy Resources in Isolated Power Systems

Phivos Therapontos, Savvas Panagi, Charalambos A Charalambous, Petros Aristidou

### Innovative Strategies for UDER Management



## Highlights

### **Coordinated Curtailment of Uncontrollable Distributed Energy Resources in Isolated Power Systems**

Phivos Therapontos, Savvas Panagi, Charalambos A Charalambous, Petros Aristidou

- Highlighting the urgency of uncontrollable distributed energy resources (UDER) curtailment for system stability
- Developing a robust Active Power Overfrequency Reduction Curve optimization framework
- Introducing a decentralized curtailment strategy for UDERs
- Validating the solution in a real-world context

# Coordinated Curtailment of Uncontrollable Distributed Energy Resources in Isolated Power Systems

Phivos Therapontos<sup>a,b</sup>, Savvas Panagi<sup>a,c</sup>, Charalambos A Charalambous<sup>b</sup>,  
Petros Aristidou<sup>c</sup>

<sup>a</sup>*Distribution System Operator, Electricity Authority of Cyprus, Nicosia, Cyprus*

<sup>b</sup>*University of Cyprus, Nicosia, Cyprus*

<sup>c</sup>*Cyprus University of Technology, Limassol, Cyprus*

---

## Abstract

The escalating integration of renewable energy sources (RES) into isolated, low-inertia power systems presents considerable challenges to maintaining frequency stability. To preserve operational security, system operators often impose stringent requirements that can necessitate RES curtailment, particularly during periods of low demand. While such measures predominantly affect large-scale distributed energy resources (DERs), prolonged curtailment scenarios may also compel output reductions from numerous small-scale, often uncontrollable, DERs (UDERs). Prevailing control strategies for UDERs typically rely on the deployment of dedicated control and communication hardware at each UDER site, incurring significant capital expenditure and implementation complexity. This paper introduces a novel methodology for the coordinated curtailment of UDERs, which circumvents the need for such supplementary equipment. The proposed approach utilizes the system frequency as an implicit communication conduit, leveraging the inherent active power-frequency (P-f) response capabilities of UDER inverters. A data-driven framework is employed to optimize a global active power-frequency reduction characteristic, tailored from historical operational data. This characteristic is subsequently implemented in a decentralized manner by individual UDERs, thereby effectively mitigating investment costs and cybersecurity vulnerabilities associated with conventional control architectures. The performance and efficacy of the proposed methodology are demonstrated through dynamic simulations on a model of the isolated, low-inertia power system of Cyprus.

*Keywords:* low inertia; uncontrollable distributed energy resources

(UDERs); frequency stability; isolated systems; renewable energy sources (RES) curtailments.

---

## 1. Introduction

Increasing awareness of environmental issues and rising electricity prices have accelerated the global adoption of Renewable Energy Sources (RES) [1]. This widespread integration of RES has introduced significant operational challenges for modern power systems, as evidenced by documented incidents of extensive load shedding that have affected thousands of consumers for extended periods [2, 3, 4]. The nature and severity of these challenges vary across power systems, influenced by factors such as network topology, the degree of RES penetration, and specific load profile characteristics.

Isolated power systems, which typically possess low rotational inertia, face heightened stability concerns, particularly in relation to frequency regulation [5]. As conventional thermal plants are gradually decommissioned and RES penetration increases, system inertia often drops below critical thresholds [6], resulting in faster frequency deviations and a greater risk of instability [7, 8, 9]. Figure 1 presents historical data from the Cyprus power system, illustrating how reduced inertia, combined with high levels of RES penetration, leads to critical values in the Rate of Change of Frequency (RoCoF).

To keep RoCoF within acceptable operational boundaries, system operators have adopted a range of stringent measures. For example, EirGrid and SONI enforce a maximum system non-synchronous penetration (SNSP) of 75%, requiring the presence of eight synchronized units, a minimum of 23,000 MW of inertia, and a 50 MW negative reserve [10]. Similarly, the Cyprus Transmission System Operator (TSOC) mandates the operation of at least four synchronous generators with a 25 MW negative reserve [11], while South Australia employs a policy of maintaining two generators on-line, supported by synchronous condensers [12].

Although these operational strategies enhance grid stability, they often result in the curtailment of renewable energy. Curtailment refers to the portion of renewable energy that goes unused due to network congestion or stability limitations [13]. Present grid codes typically require active power setpoint control only for large-scale Distributed Energy Resources (DERs), leaving smaller installations without remote control capabilities, which are categorized as Uncontrollable DERs (UDERs) [14]. The increasing presence

of UDERs presents growing security challenges in islanded systems, as these resources cannot participate in coordinated curtailment actions. As a result, developing effective management solutions for UDERs has become essential for ensuring the stability of low-inertia power systems.

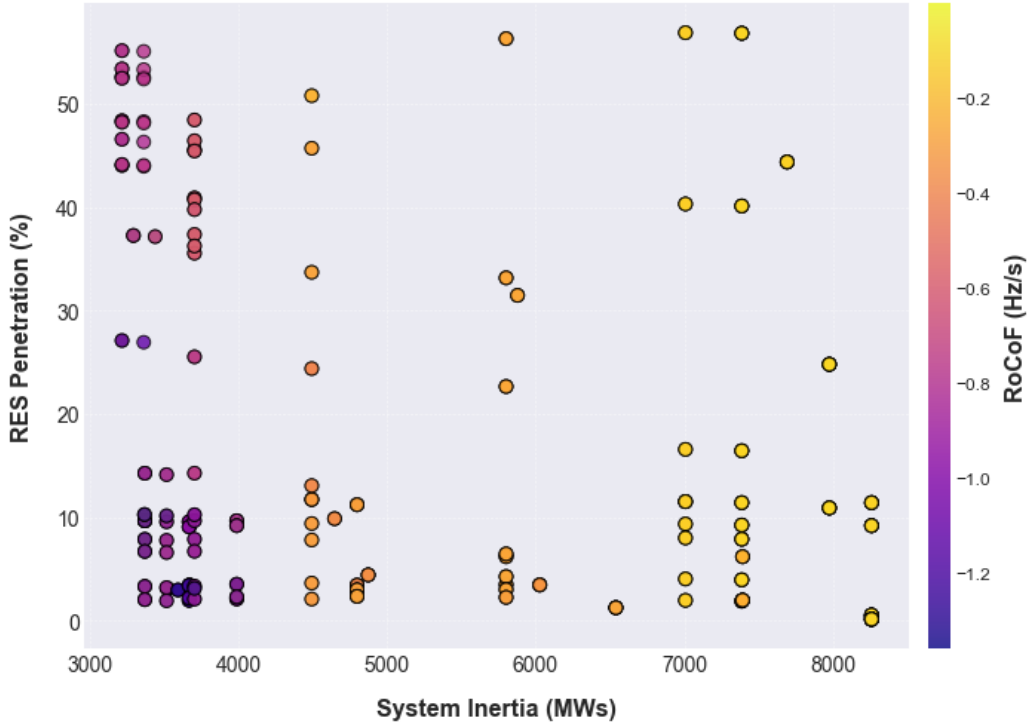


Figure 1: RoCoF variations under different inertia and RES penetration conditions

### 1.1. Motivation

In the isolated, low-inertia power system of Cyprus, the penetration of RES is substantial relative to the island’s limited load demand. During periods of low consumption, system operators frequently impose significant curtailments on renewable generation [11]. However, most installed photovoltaic (PV) systems do not support remote control, which exempts them from participating in curtailment measures. This operational gap restricts the further integration of UDERs, as their continued expansion could trigger severe frequency disturbances [14]. Therefore, developing a reliable, secure, and cost-effective approach for UDER curtailment has become a critical priority for system operators in Cyprus.

## 1.2. Literature Review

A variety of strategies have been explored for managing UDERs. Direct integration with Supervisory Control and Data Acquisition (SCADA) systems allows for precise control but requires the installation of Remote Terminal Units (RTUs) at each DER and a reliable telecommunication network, resulting in high implementation costs [14]. Ripple control technology, which employs low-frequency signal injection, offers lower deployment expenses but is limited to binary on/off operation [15]. To prevent excessive generation losses, UDERs must be grouped for coordinated switching. This grouping process is particularly challenging, as transferring a UDER from one group to another typically requires an on-site intervention. Moreover, maintaining fairness among UDER owners is essential [11]. Therefore, the system operator must monitor the estimated energy curtailed for each group to ensure an equitable allocation of curtailments across groups.

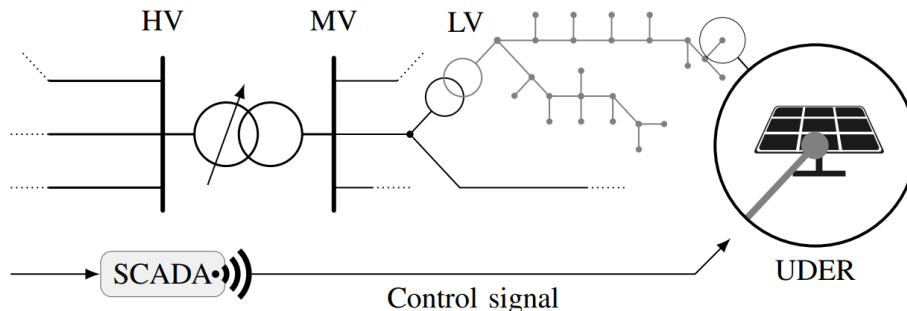


Figure 2: Communication-dependent UDER control architectures

Internet of Things (IoT)-based solutions advance beyond ripple control by supporting two-way communication and enabling dynamic reconfiguration of UDER groups. However, these systems introduce additional complexity for widely distributed assets and are exposed to ongoing cybersecurity risks [16]. Smart meters can provide disconnection functionality, yet they lack the ability to perform fine-grained curtailment and entail noticeable installation costs.

A persistent challenge is the lack of protocol standardization among inverter manufacturers. Although standards such as IEEE 2030 have been proposed, their adoption remains limited, especially among legacy devices [17, 18]. Pairing UDERs with Energy Storage Systems (ESS) can help buffer

Table 1: Comparative Analysis of UDER Curtailment Solutions

<b>Solution</b>	<b>Indicative Cost</b>	<b>Security</b>	<b>Granularity</b>
Ripple Control	€80	✓	Binary
IoT	€100	✓	Binary
Smart Meters	€100	✗	Binary
Export Limitations	€300	✓	Partial
Direct Control	N/A	✗	Full
Energy Storage Systems	> €5000	✓	Partial
SCADA	> €10000	✓	Full

surplus generation; however, this approach is often limited by economic constraints, operational coordination challenges, and regulatory barriers in European electricity markets[19, 20, 21]. For instance, during periods of low demand combined with high RES penetration, ESS units may reach full charge before the time of maximum RES output. Once saturated, the ESS can no longer absorb additional surplus energy, resulting in all excess RES generation being injected into the grid [20]. Interconnection-based solutions are ineffective for isolated grids and lose effectiveness in regions experiencing widespread photovoltaic overproduction [11].

Export limitation schemes, such as those implemented under Germany’s VDE 4105 standard, impose fixed power output caps on DERs. While straightforward, these static limits lack adaptability to changing grid conditions and can result in unnecessary curtailment of renewable energy [22]. Table 1 presents a comparative analysis of these approaches in terms of cost, security, and control granularity, while Fig. 2 illustrates the architectures that depend on communication infrastructure.

Decentralized frequency-based control schemes have emerged as promising alternatives by removing the need for communication infrastructure. Previous studies have examined coordinated load frequency response [23], adaptive frequency-watt control curves for underfrequency events [24], and frequency containment reserve strategies [14]. Despite their potential, these methods often require custom controller designs or do not fully account for interactions with synchronized units.

Based on the literature review, the currently available solutions exhibit several significant limitations. Many approaches require additional equipment and/or a robust telecommunication infrastructure, thereby increasing implementation costs and elevating cybersecurity risks. Moreover, relatively

low-cost solutions typically provide only binary control (i.e., activation or de-activation) of UDERs, which may result in inequitable curtailment allocation among participating resources.

### *1.3. Paper Contributions*

This paper addresses operational challenges in low-inertia power systems by introducing a new curtailment strategy for UDERs, utilizing the Active Power Over-Frequency Reduction Curve (APOFRC) function. The main contributions are as follows.

- **System stability and curtailment need assessment:** A quantitative analysis of historical frequency events and RES curtailments is performed to demonstrate how increasing UDER penetration impacts frequency stability in isolated systems. This analysis establishes the operational necessity for a coordinated and capability-aware UDER curtailment mechanism.
- **APOFRC optimisation framework:** A data-driven methodology is proposed for determining optimal APOFRC settings. The framework integrates clustering of representative operating conditions, dynamic simulations under credible contingencies, and a particle swarm optimisation (PSO) process. Compared to APOFRC, the framework develops a tailor-fit APOFRC considering RES curtailments.
- **Decentralised, communication-free coordination mechanism:** A frequency-shift based coordination strategy is introduced, enabling UDERs to autonomously curtail their power output using only local frequency measurements. This eliminates reliance on additional equipment or centralised curtailment commands, thereby reducing infrastructure costs and lowering cybersecurity exposure.
- **Fair and scalable curtailment allocation:** The methodology inherently allocates curtailment according to each UDERs instantaneous active power output, improving fairness compared to traditional curtailment schemes. A sensitivity analysis further demonstrates its robustness under heterogeneous APOFRC compliance.
- **Validation using real-world system models:** The full methodology is validated through detailed dynamic simulations of the Cyprus

power system under high-stress, high-UDERs penetration conditions. Results confirm that the approach enhances frequency response, reduces unnecessary curtailment, and remains effective even in mixed-inverter environments.

The structure of the paper follows this progression: Section 2 presents the theoretical background, Section 3 outlines the APOFRC design methodology, Section 4 describes the test system, Section 5 discusses the results of the implementation, and Section 6 summarizes the main findings.

## 2. Background Theory

This section provides an overview of the concepts related to Frequency Dynamics, the APOFRC, RES curtailments, and Frequency Containment Reserve (FCR).

### 2.1. Frequency Transient Dynamics

The deviation of frequency at the center of inertia,  $\Delta f(s)$ , for an active power imbalance  $\Delta P_e(s)$  is described by the transfer function in Eq. (1) [25]. This transfer function captures both the inertial and the primary frequency response dynamics of the system. The overall frequency behavior is influenced by the contribution of synchronous generators, as well as the frequency-responsive characteristics of loads and DERs. In this manuscript, emphasis is placed on how the primary frequency response of UDERs can be leveraged to reduce the active power imbalance that arises during periods of excessive RES generation.

$$G(s) = \frac{\Delta f(s)}{\Delta P_e(s)} = \left( \underbrace{(sM_s + D_s) + \sum_{i \in \Omega_s} \frac{K_i(1 + sF_iT_i)}{R_i(1 + sI_iT_i)}}_{\text{Synchronous Generators}} + \underbrace{\sum_{d \in \Omega_c^d} \frac{K_d}{R_d(1 + sI_dT_d)}}_{\text{DERs}} \right)^{-1} \quad (1)$$

Where:

- $M_s$ : Inertia
- $D_s$ : Damping
- $K_i$ : Gain of the governor of generator  $i$

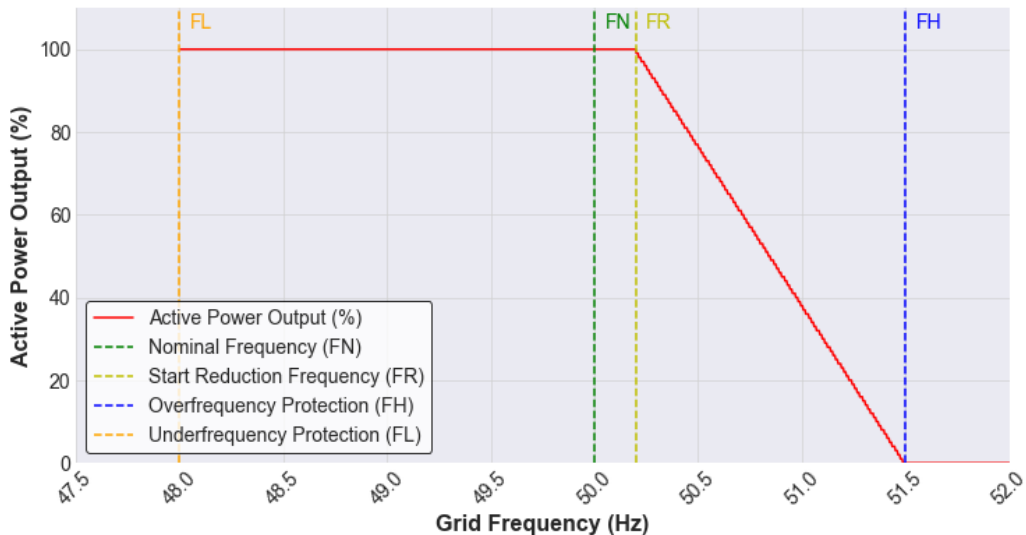


Figure 3: Representative Active Power Over-Frequency Reduction Curve (APOFRC).

- $R_i$ : Droop of the governor of generator  $i$
- $F_i T_i$ : Fast dynamics of the turbine-governor system of generator  $i$
- $I_i T_i$ : Slow dynamics of the turbine-governor system of generator  $i$
- $K_d$ : Gain of DER  $d$
- $R_d$ : Droop of DER  $d$
- $I_d T_d$ : Control-loop delay of DER  $d$

## 2.2. Active Power Over-Frequency Reduction Curve (APOFRC)

The APOFRC is a standard requirement in most grid codes and is mandatory for all DERs, irrespective of their installed capacity [26, 27, 28]. This functionality mandates DERs to reduce their active power output proportionally to deviations in system frequency measured at the PCC. As illustrated in Fig. 3, using a predefined droop characteristic, DERs begin reducing their active power output when the frequency surpasses a threshold, denoted as  $F_R$ . In instances where the system frequency falls below  $F_L$  or exceeds  $F_H$ ,

the DER unit must disconnect immediately to comply with under- or over-frequency protection protocols [29]. This mechanism enables DERs to contribute proportionally to frequency stability, thereby supporting the system in maintaining a nominal operating frequency during over-frequency events.

Figure 4 highlights how variations in APOFRC settings—specifically the frequency threshold ( $F_R$ ) and droop parameters—influence the active power output of DERs and consequently, the system’s frequency response. These settings are critical in shaping the power system’s dynamic behavior. Notably, the amount of RES penetration and the system’s available kinetic energy significantly affect the simulation results, emphasizing the importance of appropriately configuring APOFRC parameters to achieve optimal frequency response.

### 2.3. Frequency Containment Reserves

Frequency Containment Reserves (FCR) are deployed to stabilize system frequency around a designated target, typically the nominal frequency. FCR is categorized into two types: FCR normal (FCRn) and FCR disturbance (FCRd). FCRn addresses minor imbalances between generation and demand and operates without a deadband, as depicted in Fig. 5. It is specifically designed to respond to small frequency deviations within the normal operational range. Conversely, FCRd is activated when the frequency exceeds predefined normal operating boundaries, addressing larger disturbances in the power system. The proposed solution focuses on the curtailment of UDERs during standard operating conditions. Consequently, only the FCRn characteristic is considered relevant for this analysis.

### 2.4. RES Curtailment

The curtailment of RES arises from conditions such as overgeneration, the necessity to maintain minimum inertia requirements (including a minimum number of synchronized units), or elevated system non-synchronous penetration (SNSP). In regions like Cyprus and Ireland, it is estimated that more than 13% of RES energy is curtailed annually due to overgeneration [11, 13]. The extent of curtailments depends significantly on system demand, SNSP levels, and the specific technologies used in RES generation.

To ensure synchronization, all synchronized units must operate above their respective Minimum Active Power Generation Limits (MAPGL). As a result, the total system load must at least match the combined MAPGLs of all synchronized units—referred to as the Minimum Stable Generation Level

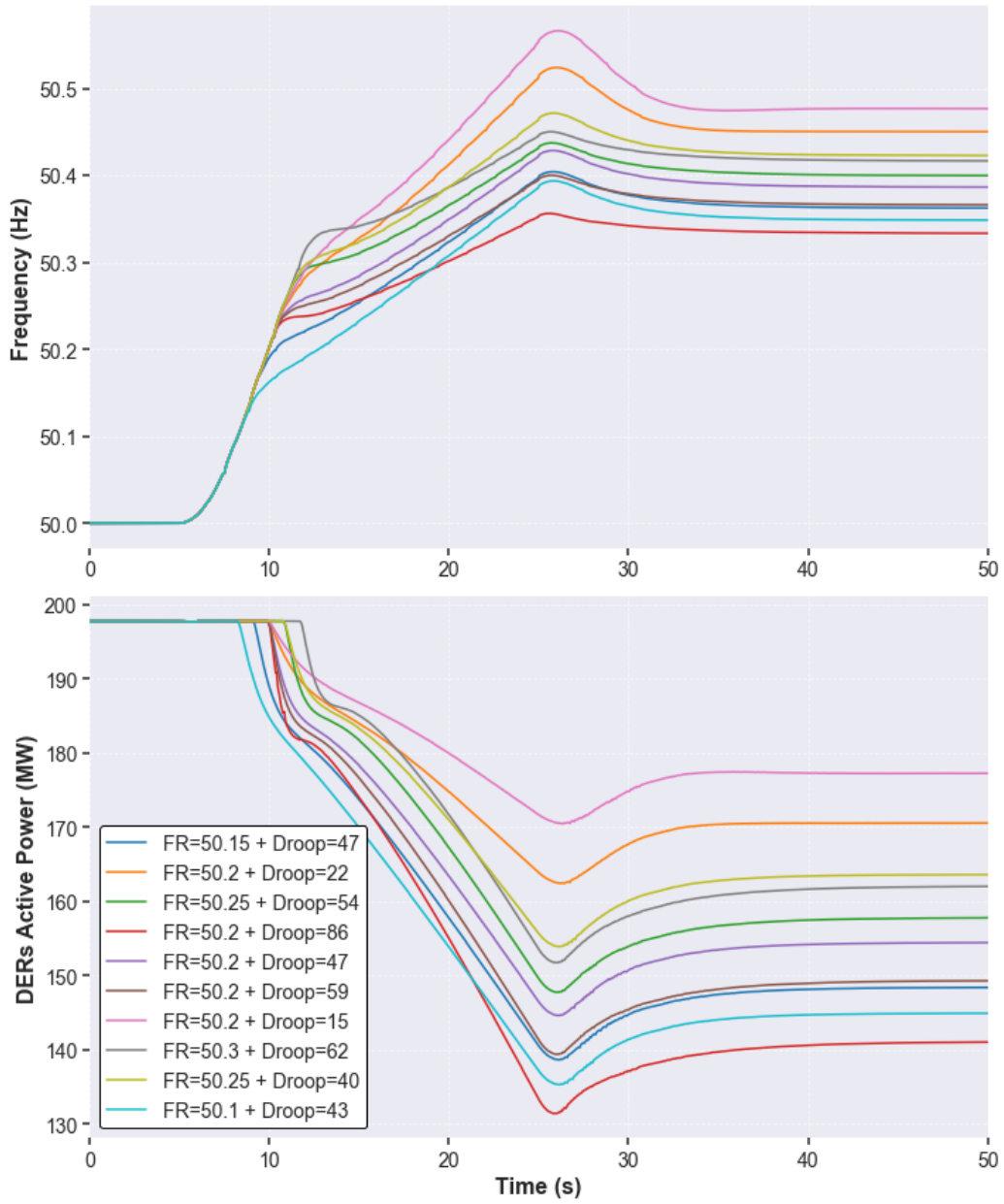


Figure 4: Impact of APOFRC frequency threshold ( $F_R$ ) and droop on DER power output and system frequency response.

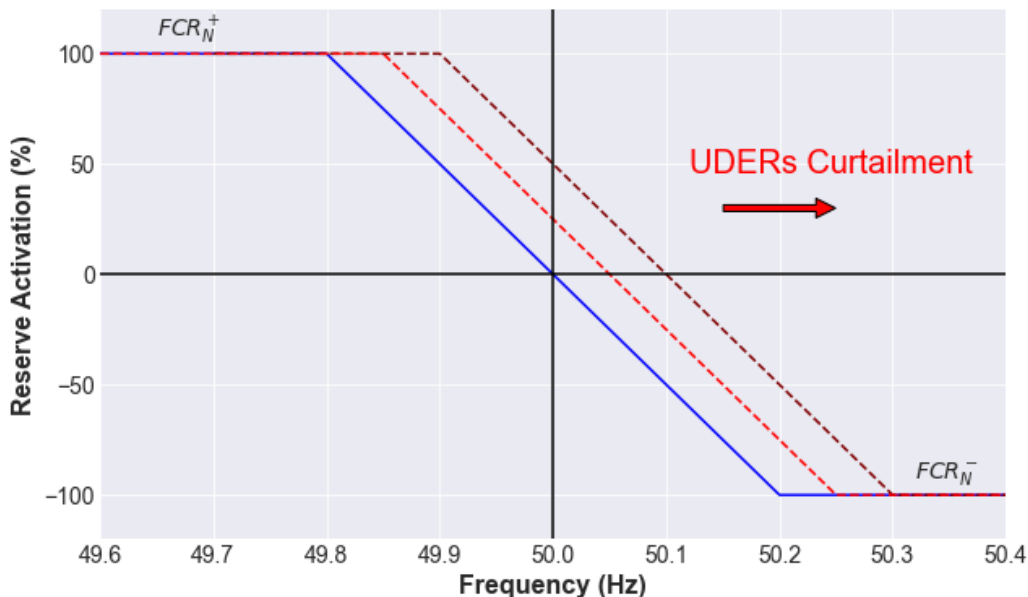


Figure 5: Frequency Containment Reserve (FCR) (Normal conditions).

(MSG L)—plus the active power contribution from DERs. During periods of low system demand, RES curtailment becomes necessary to maintain balance between generation and demand while avoiding breaches of the MSG L [11]. Curtailment is initiated when net demand falls below the MSG L of the system. Figure 6a illustrates a low-load scenario in Cyprus, where substantial RES curtailment occurs around midday due to peak RES generation coinciding with the lowest system load.

High penetration of UDERs can compromise system stability if their surplus energy cannot be adequately curtailed. Figure 6b demonstrates a scenario where, despite curtailing all controllable DERs, the increased generation from UDERs leads to an MSG L violation. This results in elevated system frequency, potentially causing a prolonged over-frequency event that could culminate in a system blackout. If further RES curtailment is required but unavailable, the system is left with two suboptimal options: disconnecting a synchronized unit or operating below the MAPGLs of synchronized units. The former reduces system inertia, while the latter risks unit desynchronization and compromises stability.

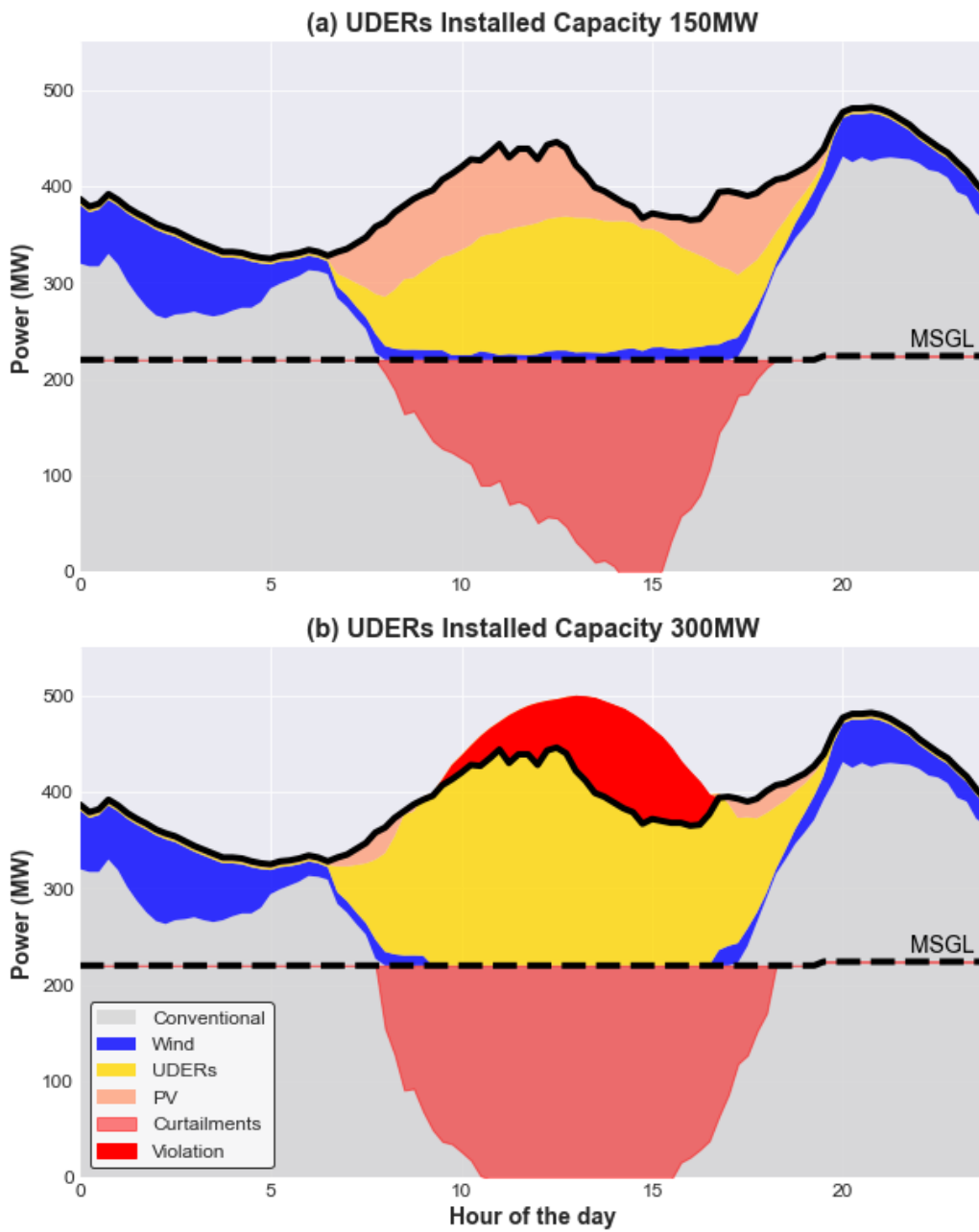


Figure 6: MSGL violation during low-load conditions with large UDER installed capacities: (a) 150 MW and (b) 300 MW.

### 3. Proposed Methodology

This section outlines the proposed methodology for developing the APOFRC and curtailing UDERs. The methodology is divided into two parts: (1) the optimization of APOFRC settings and (2) the coordinated curtailment of UDERs.

#### 3.1. Optimized APOFRC

The methodology for determining the optimal APOFRC settings is illustrated in the Algorithms 1 and 2. The process begins with the creation of simulation scenarios, as depicted in Algorithm 1. Historical data on unit commitment (UC) and economic dispatch (ED) is collected. Afterwards, operating points with zero or extremely low RES penetration are filtered out to reduce computational complexity. In this manner, only scenarios where there is an increased possibility for RES curtailment are considered. These operating points are clustered using the k-means algorithm [30], yielding representative operating conditions. The optimal number of the clusters for the k-means algorithm is identified using the silhouette analysis presented in [31]. Active power events are then defined based on TSO's specified credible contingencies. This ensures that the optimized APOFRC can maintain system frequency within nominal bounds under various operating conditions and disturbances.

---

**Algorithm 1** Simulation scenario creation for the optimized APOFRC

---

**Require:** Historical Data UC&ED, Active power events

- 1: Import UC&ED data
  - 2: Filtering operating points with extremely low RES penetration
  - 3: Silhouette analysis to identify optimal number of clusters
  - 4: K-Means clustering for data reduction
  - 5: Define simulation scenarios by applying active power events to selected operating points
- 

The representative simulation scenarios are subsequently evaluated using Algorithm 2. Initial values for  $F_R$  and droop settings are applied to all DERs, followed by root mean square (RMS)-type dynamic simulations to capture the system's frequency and active power responses accurately. After each

simulation, a Performance Index (PI) is computed using (2):

$$\begin{aligned} \text{PI} = & (F_{SS} - F_{nom}^{up}) \cdot W_{SSF} + T_{viol} \cdot W_T + \\ & (F_{Zenith} - F_{nom}) \cdot W_{Zenith} + DER_{Red} \cdot W_{DER} \end{aligned} \quad (2)$$

The PI evaluates the system's frequency response and DER active power output during disturbances. Key parameters include the steady-state frequency deviation ( $F_{SS}$ ), frequency zenith ( $F_{Zenith}$ ), duration of frequency violations ( $T_{viol}$ ), and reduction in DER energy ( $DER_{Red}$ ). Lower PI values correspond to improved system frequency response and reduced DER power losses. The weights ( $W_{SSF}, W_{Zenith}, W_T, W_{DER}$ ) are user-defined based on system characteristics, while  $F_{nom}^{up}$  represents the upper nominal frequency limit.

After analyzing all representative scenarios for specific  $F_R$  and droop settings, a Total Performance Index (TPI) is computed over the vector  $\mathbf{PI} = [PI_1, \dots, PI_N]$ , where  $N$  is the total number of simulations. The TPI is calculated using a selected norm, with the  $l_1$  norm chosen in this work to promote sparse solutions:

$$\text{TPI} = \|\mathbf{PI}\|_1 = \sum_{i=1}^N |PI_i| \quad (3)$$

---

**Algorithm 2** Development of tailored APOFRC

---

**Require:** Simulation scenarios (Algorithm 1)

- 1: Import selected simulation scenarios
  - 2: **while** PSO not completed **do**:
  - 3:     Apply  $F_R$  and Droop settings
  - 4:     Perform dynamic simulations of all scenarios
  - 5:     Compute PIs
  - 6:     Compute TPI
  - 7:     Select new  $F_R$  and Droop settings based on PSO
  - 8: **end while**
- 

The TPI serves as the objective function for the Particle Swarm Optimization (PSO) algorithm, a metaheuristic approach for nonlinear optimization [32]. PSO evaluates both individual particle and swarm-wide optimal solutions. Particle positions represent specific  $F_R$  and droop settings, which

are iteratively updated using the PSO algorithm as expressed in (4) [32]. The optimization process identifies the  $F_R$  and droop settings that minimize the TPI across all representative scenarios, ensuring an optimized APOFRC tailored to the system's requirements.

$$\begin{aligned}
u_i(t+1) &= w \cdot u_i(t) + c_1 \cdot r_1 \cdot (p_i^{\text{best}} - APOFRC_i(t)) \\
&\quad + c_2 \cdot r_2 \cdot (g^{\text{best}} - APOFRC_i(t)) \\
APOFRC_i(t+1) &= APOFRC_i(t) + u_i(t+1)
\end{aligned} \tag{4}$$

**Where:**

- $u_i(t+1)$ : velocity of particle  $i$  at iteration  $t+1$
- $u_i(t)$ : velocity of particle  $i$  at iteration  $t$
- $w$ : inertia weight
- $c_1$ : cognitive coefficient
- $c_2$ : social coefficient
- $r_1, r_2$ : random numbers uniformly distributed in  $[0, 1]$
- $p_i^{\text{best}}$ : best position of particle  $i$
- $g^{\text{best}}$ : global best position
- $APOFRC_i(t)$ : APOFRC settings ( $F_R$  and  $Droop$ ) of particle  $i$  at iteration  $t$
- $APOFRC_i(t+1)$ : APOFRC settings ( $F_R$  and  $Droop$ ) of particle  $i$  at iteration  $t+1$

### 3.2. Coordinated Curtailment of UDEs

The proposed methodology for curtailing the active power of UDEs leverages the optimized APOFRC and frequency as a coordination signal. This approach builds upon the authors' previous work [14]. Under normal operating conditions, power system frequency is tightly regulated around the nominal value, with control mechanisms assuming a nominal frequency as the desired operating point. However, by intentionally shifting the frequency set-point for controlled units (both synchronous and asynchronous), the system

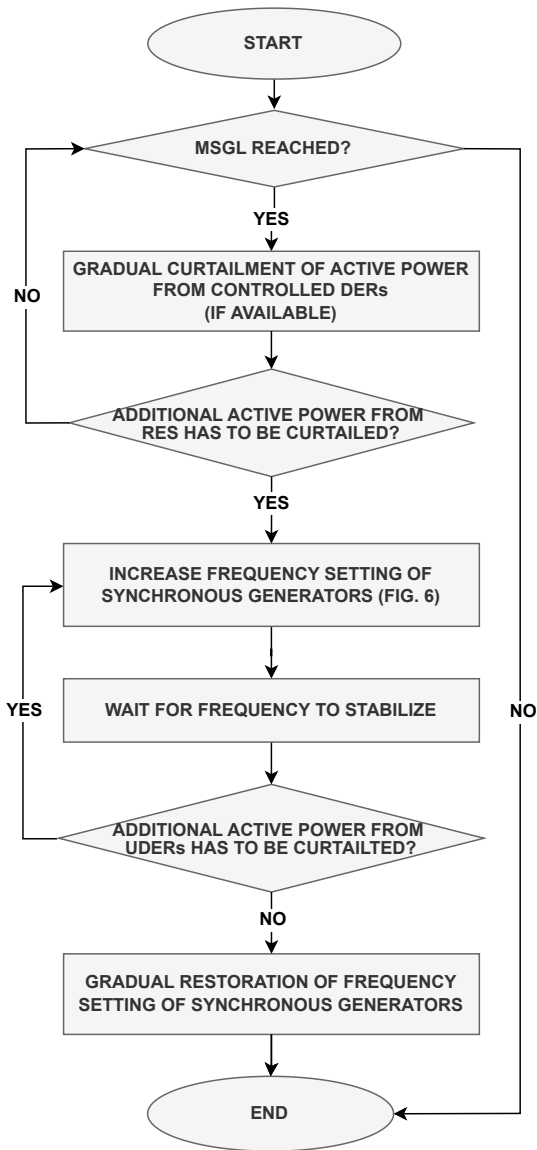


Figure 7: Coordination strategy for the proposed UDER curtailment methodology.

can drive UDERs into their curtailment region as defined by the APOFRC. This involves setting the system frequency above  $F_R$ , as illustrated in Fig. 3.

When curtailment of UDERs is required, SCADA-controlled units participating in frequency balancing are provided with a new frequency setpoint. This action effectively shifts their FCR curves to the right, allowing the system frequency to increase in a controlled manner, as shown in Fig. 5. As the system frequency surpasses  $F_R$ , UDERs begin to curtail their active power output. This approach ensures the system operates at a higher—but still acceptable—frequency, thereby inducing UDERs to enter their curtailment region.

The coordination strategy is illustrated in Fig. 7. When the MSGL is reached, the system operator first issues active power setpoints to all controlled DERs. In this way, the required active power reduction is gradually achieved through controlled DER curtailments. The analytical description for curtailing controllable DERs in Cyprus is available in [11]. If additional curtailment is still required after all controlled DERs have reached their minimum active power output, the system frequency setpoint is incrementally increased, thereby driving UDERs into their curtailment region. Appropriate delays between successive frequency setpoint adjustments are incorporated to ensure system stability.

Conversely, when the reduction of active power from UDERs is no longer required, the frequency setpoints of SCADA-controlled units are gradually increased. When the system frequency falls below  $F_R$ , UDER curtailment ceases. Although not explicitly shown in Fig. 7, the curtailment of controllable DERs is similarly reduced when net load exceeds the MSGL, thereby restoring system balance.

## 4. Case Study Description

This section evaluates the methodologies introduced in Section 3 through targeted case studies. The evaluation is divided into two parts: (1) assessing the optimal settings for the APOFRC, and (2) analyzing the coordinated curtailment of UDERs. An overview of the Cyprus power system is also provided to contextualise the case studies.

### 4.1. Power System of Cyprus

The proposed methodologies were tested on the Cyprus power system, modelled using data provided by TSOC. Cyprus operates as a low-inertia,

isolated system with a nominal frequency of 50 Hz. The total conventional generation capacity is 1478 MW, distributed across three major power plants. RES penetration exceeds 25%, calculated as the ratio of total RES-generated energy to total energy consumption. The system includes more than 900 MW of installed PV capacity and 170 MW of wind power [33]. Additionally, the system incorporates 400 MW of UDERs, of which 250 MW are equipped with ripple and IoT receivers, and the remaining are SCADA-connected controllable DERs.

Simulations were conducted using DIgSILENT PowerFactory software [34]. Generic models for PV and wind power plants (WPP) compliant with the WECC standard were employed to ensure adherence to grid code requirements [35]. DERs were modeled following the Cypriot grid code, which is based on the German VDE4105 standard [26].

#### 4.2. Optimized APOFRC

The parameters used to calculate the Performance Index (PI) for evaluating APOFRC settings are summarised in Table 2.

Table 2: Performance Index Parameter Values

Parameter	Acronym	Value
Nominal Frequency	$F_{nominal}$	50 Hz
Maximum Nominal Frequency	$F_{nominal}^{up}$	50.2 Hz
Steady-State Frequency Weight	$W_{SSF}$	5000
Frequency Zenith Weight	$W_{Zenith}$	1000
Frequency Violation Duration Weight	$W_t$	1000
DER Reduction Weight	$W_{DER}$	1

To balance computational efficiency with accuracy, the PSO algorithm parameters were selected based on commonly used values in the literature [36]. The parameters included an inertia weight ( $w = 1$ ), acceleration coefficients ( $c_1 = c_2 = 2$ ), a swarm size of 20, and parameter constraints:  $F_R$  ranging from 50.2 Hz to 50.3 Hz, and droop ranging from 20% to 100% (p.u./Hz).

The study utilized 15-minute historical UC and ED data from the Cyprus power system for the year 2022. To focus on scenarios with significant penetration of RES, operating points with RES generation greater than 100 MW were filtered and analyzed. Using silhouette analysis and the k-means algorithm, 100 representative operating points were selected.

Furthermore, credible contingencies, defined as 8% and 16% of total system load, were incorporated into the analysis based on TSOC data. These contingencies included both ramp and step events. The combination of representative operating points and predefined contingencies formed the basis for the simulation scenarios.

#### 4.3. Coordinated Curtailment of UDERs

To evaluate the effectiveness of the proposed methodology for curtailing UDERs using the custom-fit APOFRC the operating condition from the lower demand of 2022 (450 MW occurred in April) was utilised. The analysed generation profile is presented in Fig. 6(b). In this scenario, the total installed capacity of the UDERs is increased to 300MW compared to the 150MW shown in Fig. 6(a). The analysis is focused at 14:00, which is the time when the MSGL has the largest violation.

At that time, four synchronized units (Steam Turbines) are operating at their minimum stable generation limits. As it can be seen in Fig. 6(b) the controllable DERs have been fully curtailed. The controllable DERs have been curtailed with zero setpoint instructions from the SCADA system of the system operator. As mentioned in the introduction, disconnecting a generator is not allowed, in order to maintain RoCoF values within acceptable limits.

To evaluate the effectiveness of the methodology for future scenarios with increased UDERs penetration a sensitivity analysis was performed. Thus, the installed capacity of UDERs has been increased from 300 MW to 900 MW with a 150 MW increase in each simulation. In addition, a sensitivity analysis has been performed considering UDERs with heterogeneous APOFRC compliance.

## 5. Results

This section presents and analyzes the results of the case studies. The first part focuses on developing the optimized APOFRC, while the second part evaluates the proposed methodology for curtailing UDERs.

### 5.1. Optimized APOFRC

Using the methodology detailed in Section 3, the optimal settings of APOFRC were calculated as  $F_R = 50.2$  Hz and Droop = 100% (Fig. 8).

The examined settings, determined through the PSO, and their corresponding normalized TPI values are also shown in Fig. 8. For lower values of  $W_{DER}$ , the TPI decreases as  $F_R$  decreases and Droop increases. This trend reflects the relationship described by (2), where the individual PI increases when the system's frequency response deviates from the nominal limits.

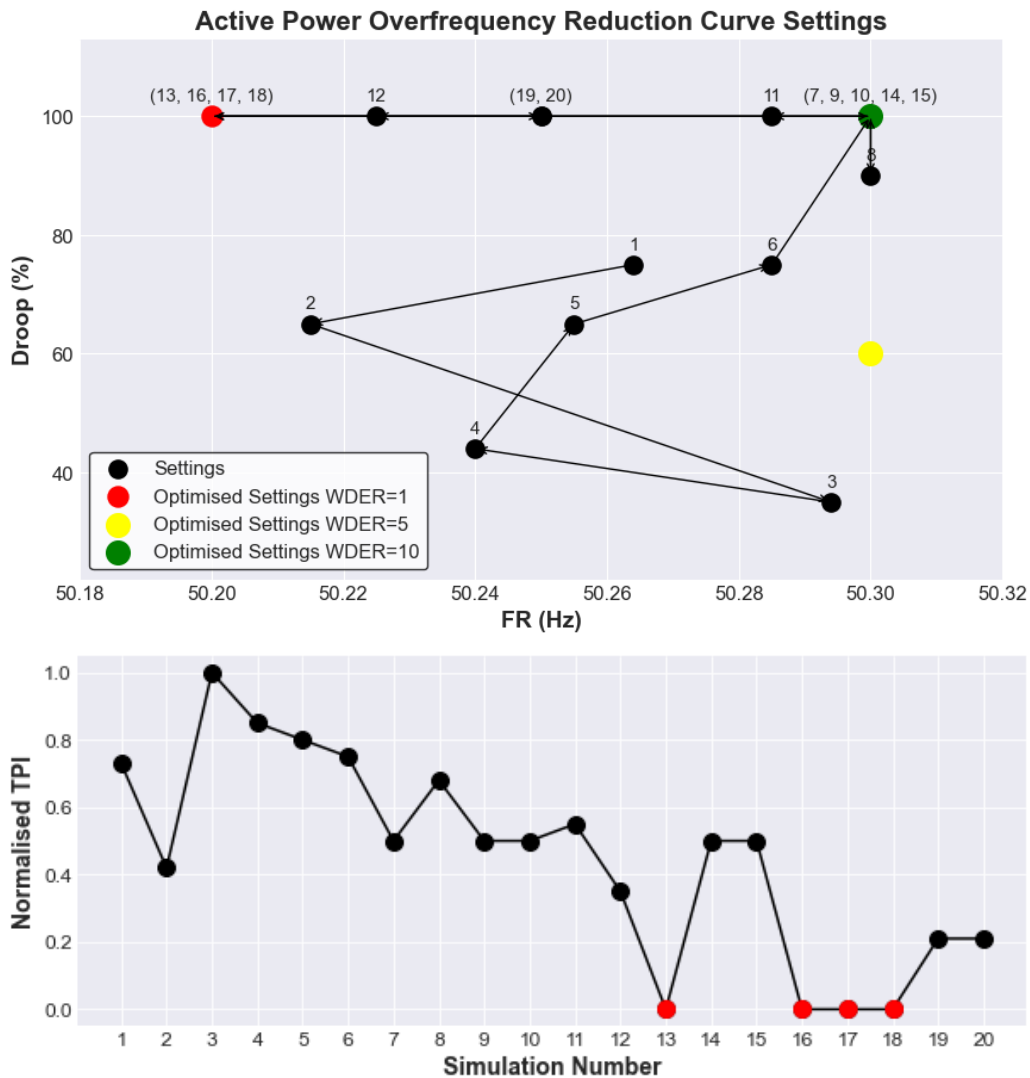


Figure 8: Evaluated APOFRC settings and variation of normalized TPI.

The optimized APOFRC settings exhibit a strong dependency on the

value of  $W_{DER}$ , the weight assigned to the curtailed energy of DERs. This dependency is highlighted in Fig. 8. When  $W_{DER}$  increases from 1 to 5, the optimal settings shift to  $F_R = 50.3$  Hz and Droop = 60% (yellow dot). Similarly, when  $W_{DER}$  is set to 10, the optimal settings become  $F_R = 50.3$  Hz and Droop = 100% (green dot). This behavior occurs because  $W_{DER}$  drives the PSO algorithm to prioritise reducing RES curtailments, allowing greater frequency excursions.

Figure 9 illustrates the system frequency response for all evaluated operational scenarios, considering a disturbance equivalent to 10% of the total system load and using the optimal APOFRC settings. The results demonstrate that the optimized settings effectively contain frequency excursions within acceptable limits, ensuring an adequate frequency response under diverse operating conditions.

### 5.2. Coordinated Curtailment of UDERs

This subsection evaluates the effectiveness of the proposed methodology for curtailing UDERs. Initially, the optimized APOFRC settings were applied to all UDERs, and the required UDER curtailments for each simulation were calculated, as shown in Fig. 10. The results indicate that the needed curtailments increase proportionally with the installed UDER capacity. Simultaneously, all available controllable DERs are fully curtailed, as also depicted in Fig. 10. This outcome is expected, as the system operator initially curtails all active power from controllable DERs to prevent violations of the MSG. However, in this case study, the low load demand combined with high UDER installed capacity necessitates additional curtailments.

In Fig. 11 the system's frequency response and the active power response of UDERs during the analysis are illustrated. At  $t = 10$  s, a new frequency setpoint of 50.3 Hz is sent to the SCADA-controlled units participating in frequency balancing. As a result, the system frequency is allowed to increase. UDERs, equipped with the tailored APOFRC curve, begin reducing their active power output once the system frequency exceeds  $F_R$  (50.2 Hz). Throughout the analysis, all synchronized units consistently operate above their MAPGLs.

The results confirm that the proposed methodology successfully fulfills UDER curtailment requirements. Even under the most challenging scenario of 900 MW UDER installed capacity, the system frequency stabilizes slightly above the shifted nominal limit. These findings demonstrate that the pro-

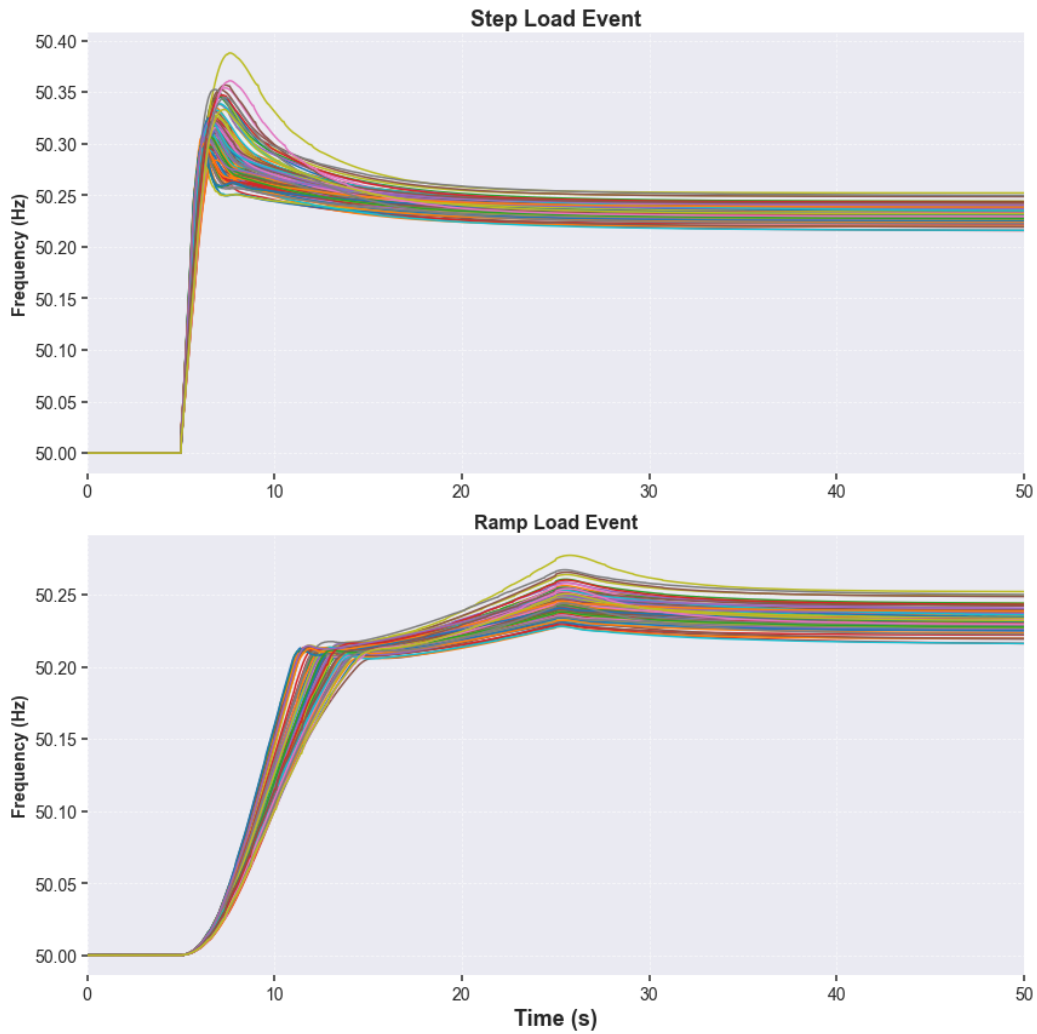


Figure 9: System frequency response with the optimal APOFRC settings.

posed methodology can effectively curtail UDERs without requiring additional equipment or infrastructure.

In addition, a sensitivity analysis was performed to demonstrate how the proposed methodology performs when DERs have different APOFRC settings from the optimal. The analysis considered three different type of UDERs:

- Optimal: UDERs equipped with the optimal APOFRC

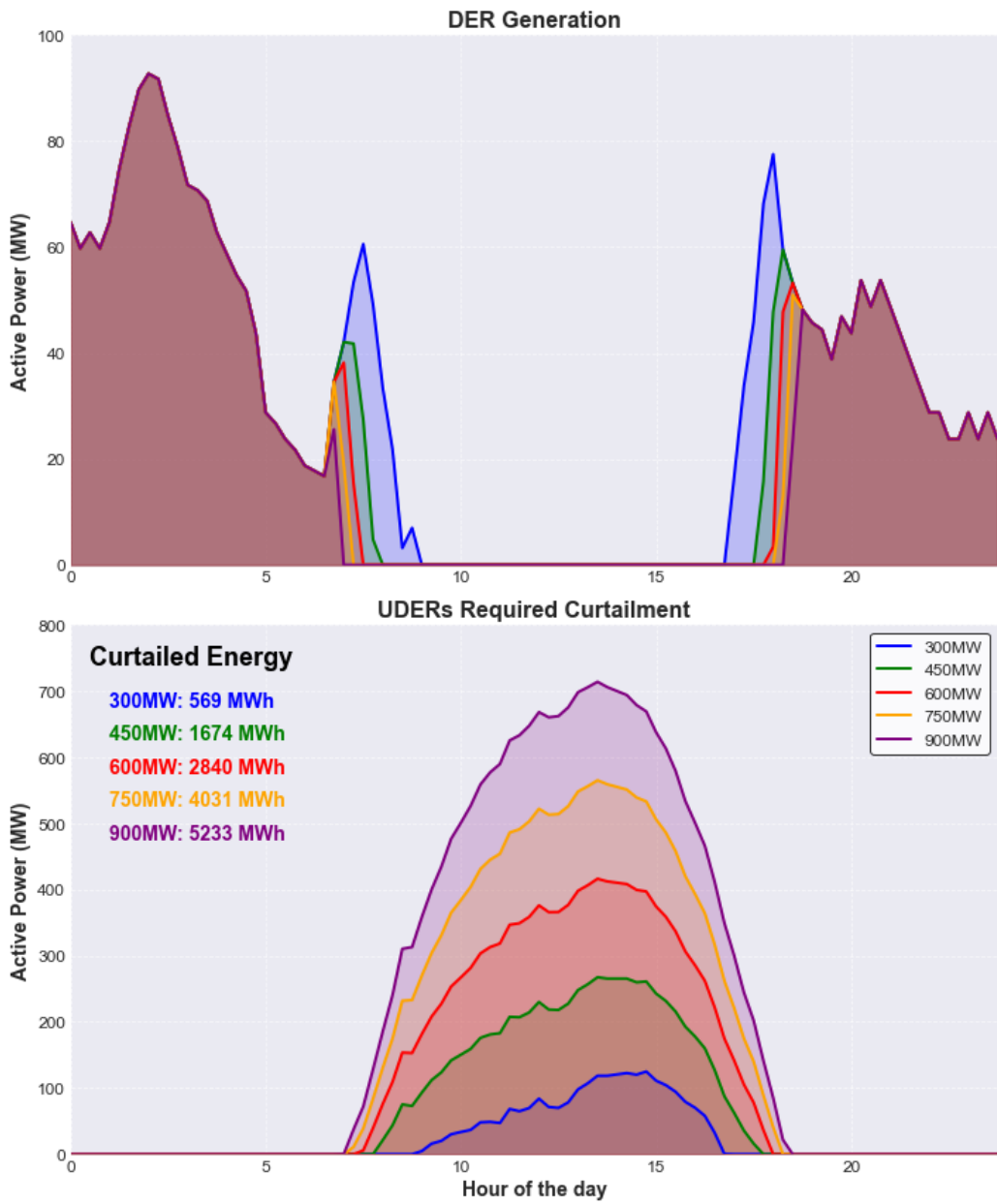


Figure 10: Controllable DER generation and required UDER curtailment.

$Dr\text{oop} = 100\%$  and  $F_R = 50.2$  Hz

- Reference: UDERs with APOFRC

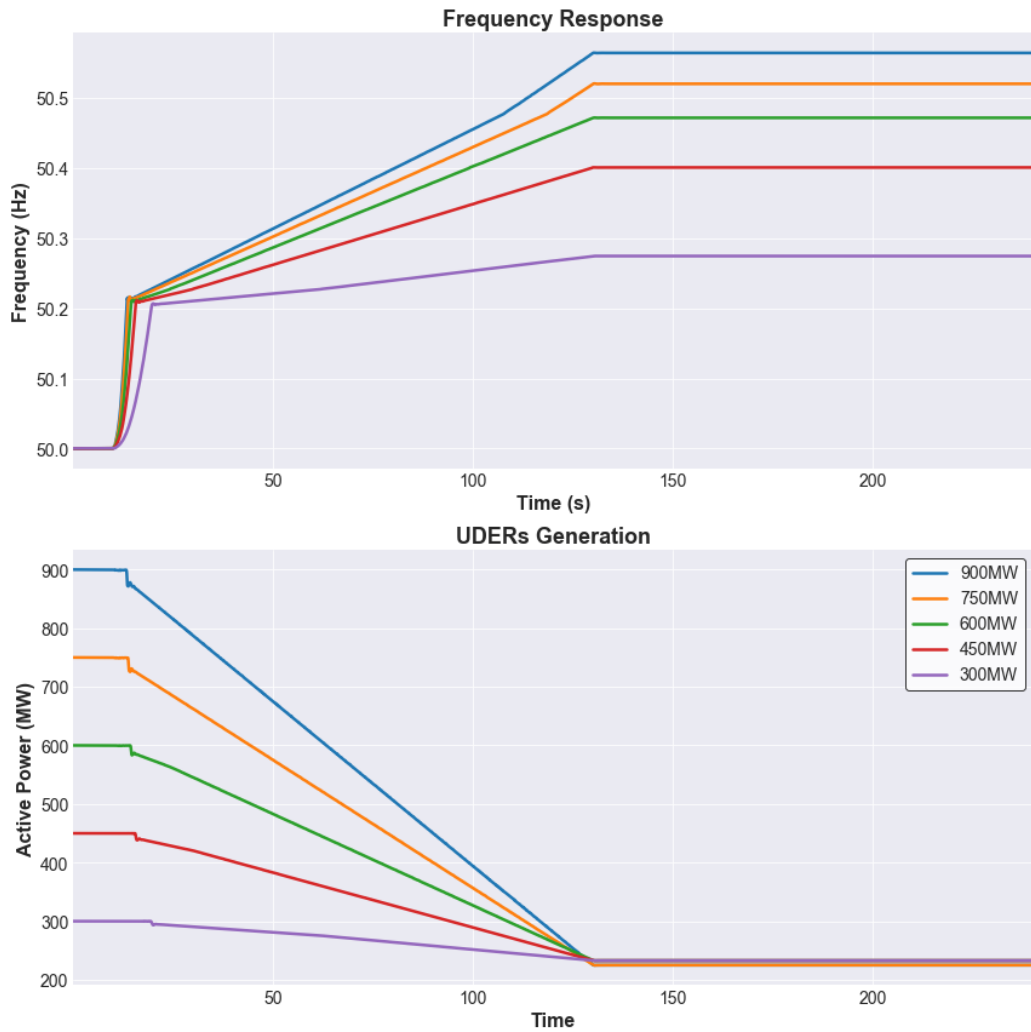


Figure 11: Frequency response and active power response from UDERs.

$$Droop = 50\% \text{ and } F_R = 50.2 \text{ Hz}$$

- No APOFRC: UDERs without APOFRC capability

In each scenario presented in Table 3, the proportion of DERs equipped with each type of APOFRC varies. For the analysis, the total installed capacity of UDERs was fixed at 600 MW. The corresponding results are illustrated in Fig. 12 and summarised in Table 3.

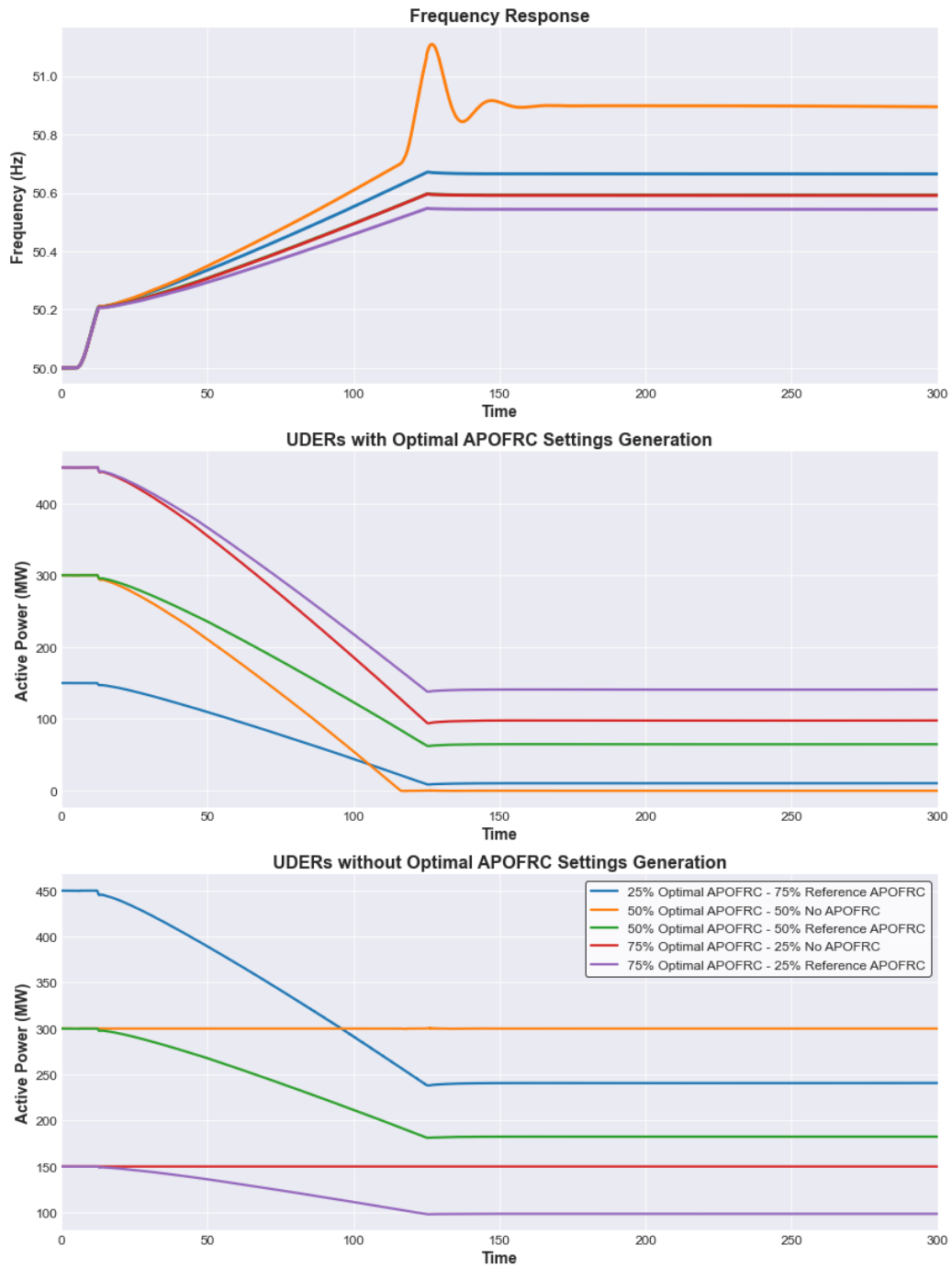


Figure 12: Frequency response and active power response from UDERs for different APOFRC.

The analysis indicates that the proposed methodology can be applied to curtail UDERs even when not all DERs are equipped with the optimal APOFRC. However, as the penetration of UDERs without optimal APOFRC increases, the resulting steady-state frequencies also rise. Consequently, the effectiveness of the methodology diminishes as the number of non-optimal UDERs grows. Furthermore, when the share of UDERs without APOFRC exceeds 25%, the frequency response noticeably deteriorates, with the maximum frequency reaching 51.1 Hz instantaneously. This is due to the fact that all the available active power from UDERs with Optimal settings has been exhausted before satisfying the required curtailments. It should be noted that this scenario is highly improbable, as APOFRC requirements have been incorporated into major grid codes for more than a decade.

Additionally, as the penetration of UDERs with the optimal APOFRC decreases, their corresponding curtailments increase. This occurs because UDERs lacking the optimal curve provide limited or no contribution to frequency containment. Consequently, UDERs with higher Droop values reduce their active power output more aggressively, resulting in an unfair distribution of curtailments among UDERs.

Table 3: Impact of APOFRC on UDERs curtailment and steady state frequency

<b>SCENARIO</b>	<b>UDERs with Optimal APOFRC Curtailed</b>	<b>UDERs with Reference APOFRC Curtailed</b>	<b>Steady State Frequency</b>
100% Optimal	365 MW	0 MW	50.48 Hz
75% Optimal & 25% Reference	310 MW	52 MW	50.54 Hz
75% Optimal & 25% No APOFRC	352 MW	0 MW	50.59 Hz
50% Optimal & 50% Reference	235 MW	117 MW	50.59 Hz
50% Optimal & 50% No APOFRC	290 MW	0 MW	50.90 Hz
25% Optimal & 75% Reference	135 MW	210 MW	50.67 Hz

## 6. Conclusions

As RES penetration increases, curtailments during low-load demand periods are becoming a critical challenge, particularly in low-inertia, isolated power systems. These systems face heightened operational constraints to maintain stability, and under extremely low demand conditions, the need to curtail active power from UDERs arises. However, existing solutions require additional equipment for each UDER, and rely on robust communication systems, which are not always feasible or cost-effective.

In this work, a novel methodology for curtailing UDERs without additional equipment or extensive telecommunication infrastructure has been introduced. The proposed solution minimizes cybersecurity risks and eliminates the complexities associated with managing a large number of DERs. By leveraging the inherent capabilities of the APOFRC embedded in DER inverters, this methodology provides a practical, scalable, and secure alternative. Furthermore, the proposed solution incorporates a fairness principle among UDER owners by ensuring that all units (equipped with optimal APOFRC) experience an equal proportional reduction in curtailment.

A secondary but equally significant contribution of this work is the development of an optimisation framework to identify APOFRC settings. This framework uses historical operational data and the PSO algorithm to compute settings that balance system performance with minimal RES curtailment. This optimisation ensures a stable frequency response under varying scenarios, making the approach robust and adaptable.

The applicability and effectiveness of the proposed methodologies were validated on the low-inertia, isolated power system of Cyprus. The results demonstrated that: 1) Optimal APOFRC settings significantly enhance system stability and frequency containment during over-generation events; and, 2) The proposed curtailment methodology effectively addresses UDER management challenges, even under high installed capacities, without requiring additional infrastructure.

The contributions of this work extend beyond the Cyprus case study. The proposed UDER curtailment methodology is versatile and can be deployed in any isolated power system, providing a cost-effective solution in scenarios where advanced communication systems or additional equipment are unavailable. It is particularly suitable for developing countries, where financial constraints may hinder the deployment of complex DER management systems. Nevertheless, it is recommended that this methodology be

considered a transitional solution. As inverter communication protocols mature and cyber security frameworks are enhanced, more advanced control systems will become viable. Until then, the proposed approach offers a secure and efficient pathway for increasing RES penetration while maintaining power system stability.

On the other hand, the proposed methodology exhibits certain limitations. It requires a comprehensive and accurate power system model that includes, at a minimum, the dynamic controls of synchronous generators and UDERs equipped with APOFRC. Moreover, as demonstrated in the sensitivity analysis on the penetration of UDERs with the optimal APOFRC, the methodology becomes more effective and equitable as the number of UDERs employing the optimal curve increases. Consequently, applying the optimal APOFRC to as many UDERs as possible is recommended, although achieving this in practice may pose challenges for both system operators and UDER owners.

Conclusively, this work provides an innovative, practical, and resource-efficient solution to a critical challenge in modern power systems. By addressing both technical and economic barriers, it lays the groundwork for scalable and sustainable integration of DERs in isolated power systems.

## 7. Acknowledgments

This project has received funding from the EU's Horizon Europe Framework Programme (HORIZON) under the GA n. 101120278 -DENSE

## References

- [1] International Renewable Energy Agency (IRENA), Renewable energy highlights (2024).
- [2] J. Wachter, L. Gröll, V. Hagenmeyer, Survey of real-world grid incidents—opportunities, arising challenges and lessons learned for the future converter dominated power system, *IEEE Open Journal of Power Electronics* (2023).
- [3] National Grid ESO, Technical report on the events of 9 August 2019 (2019).

- [4] Australian Energy Market Operator (AEMO), Black System South Australia 28 September 2016 (2017).
- [5] F. Milano, F. Dörfler, G. Hug, et al., Foundations and challenges of low-inertia systems, in: 2018 Power Systems Computation Conference (PSCC), 2018.
- [6] S. Panagi, P. Aristidou, Sizing of fast frequency response reserves for improving frequency security in low-inertia power systems, Sustainable Energy, Grids and Networks (2025).
- [7] N. Hatziargyriou, J. Milanovic, C. Rahmann, et al., Definition and classification of power system stability—revisited & extended, IEEE Transactions on Power Systems (2020).
- [8] M. Rampokanyo, P. Dattaray, P. Kamera, et al., Impact of high penetration of inverter-based generation on system inertia of networks, Electra (2021).
- [9] ENTSOE, Rate of change of frequency withstand capability (2018).
- [10] EirGrid and SONI, Potential solutions for mitigating technical challenges arising from high RES-E penetration on the island of Ireland (2021).
- [11] P. Therapontos, R. Tapakis, P. Aristidou, et al., RES curtailments in Cyprus: A review of technical constraints and solutions, Solar Energy Advances (2025).
- [12] F. Arraño-Vargas, Z. Shen, S. Jiang, et al., Challenges and mitigation measures in power systems with high share of renewables—the Australian experience, Energies (2022).
- [13] EirGrid and SONI, Annual renewable energy constraint and curtailment report (2023).
- [14] P. Therapontos, A. Stavrou, P. Aristidou, Increasing hosting capacity of uncontrollable distributed energy resources in isolated power systems, in: 2023 IEEE ISGT Europe, 2023.

- [15] D. Dzung, I. Berganza, A. Sendin, Evolution of powerline communications for smart distribution: From ripple control to OFDM, in: 2011 IEEE International Symposium on Power Line Communications and Its Applications, IEEE, 2011.
- [16] Q. Wang, G. Zhang, F. Wen, A survey on policies, modelling and security of cyber-physical systems in smart grids, IET Energy Conversion and Economics (2021).
- [17] D. Vaidhynathan, K. Prabakar, A. Singh, et al., Enabling interoperable SCADA communications for PV inverters through embedded controllers, Tech. rep., National Renewable Energy Lab.(NREL) (2021).
- [18] D. Passos, C. de Sousa, R. C. Gomes, et al., A tutorial and security overview on the IEEE 2030.5-2018 standard, IEEE Communications Surveys & Tutorials (2025).
- [19] H. Grover, T. Verna, A. Bhatti, A fast and robust dobc based frequency and voltage regulation scheme for future power systems with high renewable penetration, IET Energy Conversion and Economics (2023).
- [20] K. Petrou, L. F. Ochoa, A. T. Procopiou, et al., Limitations of residential storage in PV-rich distribution networks: An Australian case study, in: IEEE General Meeting 2018, IEEE, 2018.
- [21] Journal of the European Union, DIRECTIVE (EU) 2019/944 (2019).
- [22] K. Petrou, A. T. Procopiou, L. Gutierrez-Lagos, M. Z. Liu, L. F. Ochoa, T. Langstaff, J. M. Theunissen, Ensuring distribution network integrity using dynamic operating limits for prosumers, IEEE Transactions on Smart Grid 12 (5) (2021) 3877–3888.
- [23] H. Mavalizadeh, L. A. D. Espinosa, M. R. Almassalkhi, Improving frequency response with synthetic damping available from fleets of distributed energy resources, IEEE Transactions on Power Systems (2023).
- [24] H. D. Tafti, G. Konstantinou, Q. Lei, et al., Adaptive power system frequency support from distributed photovoltaic systems, Solar Energy (2023).

- [25] A. M. Nakiganda, S. Dehghan, U. Markovic, G. Hug, P. Aristidou, A stochastic-robust approach for resilient microgrid investment planning under static and transient islanding security constraints, *IEEE transactions on smart grid* 13 (3) (2022) 1774–1788.
- [26] VDE, Power generating plants in the low voltage network (VDE-AR-N 4105) (2019).
- [27] AUSTRALIAN/NEW ZEALAND STANDARD, Grid connection of energy systems via inverters, Part 2: Inverter requirements (2020).
- [28] IEC, Requirements for generating plants to be connected in parallel with distribution networks - Part 1: Connection to a LV distribution network - Generating plants up to and including Type B (EN50549-1) (2023).
- [29] S. Xu, Y. Xue, L. Chang, Review of power system support functions for inverter-based distributed energy resources-standards, control algorithms, and trends, *IEEE Open journal of Power Electronics* (2021).
- [30] F. Pedregosa, G. Varoquaux, A. Gramfort, et al., Scikit-learn: Machine learning in python, *Journal of Machine Learning Research* (2011).
- [31] S. M. Miraftabzadeh, C. G. Colombo, M. Longo, F. Foiadelli, K-means and alternative clustering methods in modern power systems, *IEEE Access* 11 (2023) 119596–119633.
- [32] J. Kennedy, R. Eberhart, Particle swarm optimization, in: *International conference on neural networks*, IEEE, 1995.
- [33] Transmission System Operator of Cyprus (TSOC), Ten-year development plan (2023-2032) (2022).
- [34] DIgSILENT GmbH., PowerFactory 2024 - User manual (2024).
- [35] G. Lammert, L. D. P. Ospina, P. Pourbeik, et al., Implementation and validation of wecc generic photovoltaic system models in digsilent powerfactory, in: *IEEE General Meeting 2016*, 2016.
- [36] D. Wang, D. Tan, L. Liu, Particle swarm optimization algorithm: An overview, *Soft computing* (2018).